Feedback Linearization-Based Satellite Attitude Control with a Life-Support Device without Communications

Alessandro Giuseppi [1,*], Antonio Pietrabissa [1]

Samuele Cilione [2], Luigi Galvagni [2]

[1] *Sapienza, University of Rome, Department of Computer, Control And Management Engineering "Antonio Ruberti" (DIAG) Via Ariosto 25, Rome, 00185, Italy.*

[2] *Thales Alenia Space Italia, Department of Guidance Navigation & Control Engineering Via Saccomuro 24, Rome, 00131, Italy*

Abstract: This paper develops a control strategy for a life-support device to be attached to an orbiting satellite to extend its operational life. The objective is met in such a way that the original satellite keeps operating without communications between the two systems (also valuable for energy efficiency). The case in which the original satellite is equipped with a feedback-linearization based controller is considered and the control law for the life-support is developed with the same methodology, obtaining a compensating control which recovers the performance of the original control strategy. Simulations validate the approach considering a real case study in various scenarios.

Key Words: Satellite systems, spacecraft attitude control, feedback linearization, model predictive control.

Nomenclature	
$\times, \cdot, \otimes$	Vector, scalar and cross products
C	Control horizons of Model Predictive Control
$\boldsymbol{I_n}$	$(n \times n)$ identity matrix
$\boldsymbol{J_B}$	Moment of Inertia (MOI) tensor
I_x, I_y, I_z	Principal MOIs
K	Gain for momentum unloading
$\boldsymbol{L_w}, \boldsymbol{L_{wn}}$	Angular momentum of the reaction wheels for the satellite and the life-support system
$L_f h(x)$	Lie derivative of $h(x)$ along f
$m_1, l_1, \boldsymbol{J^1}$	Mass, edge length and MOI tensor for the satellite
$m_2, l_2, \boldsymbol{J^2}$	Mass, edge length and MOI tensor for the life-support system
P	Prediction horizon of Model Predictive Control
$\boldsymbol{q}, \boldsymbol{q_{13}}, q_4$	Quaternion representation of the attitude, vector and scalar components of the quaternion
$\boldsymbol{q^{ref}}$	Reference quaternion
$\boldsymbol{Q}$	Error weight matrix of the controller
$\boldsymbol{R}$	Control weight matrix of the controller
T	Time constant of the reference
$\boldsymbol{x} = [\boldsymbol{q}\ \boldsymbol{\omega}]^T$	State vector
$\boldsymbol{\delta}$	Error quaternion representation of the attitude
$\boldsymbol{\tau}$	External torques
$\boldsymbol{\tau_w}, \boldsymbol{\tau_{wn}}$	Torques applied by the reaction wheels of the satellite and of the life-support system
$\boldsymbol{\omega}$	Angular velocity of the inertial reference frame relative to the satellite measured in its coordinates

1 Introduction

Prolonging the satellite operation life is becoming a crucial topic in spacecraft research, as it is related to the reduction of space debris, which is one of the main issues that modern space systems is facing (Liou, 2006). In fact, modern satellite mission planning should take into account not only orbital and attitude control, but also the disposal of the device once its operation life is elapsed. For this reason, this paper envisages the development of a control strategy for the operation of a "life-support" system that can be attached to an orbiting satellite to either extend its operational life once its propellant, or in general the lifetime of some of its components, has been depleted or to provide the satellite with new, updated, equipment, with immediate economic benefits for the spacecraft operator.

The considered life-support system is equipped with a set of reaction wheels, the typical actuator in attitude control problems, and a set of thrusters that may replace the depleted ones of the satellite for the required procedure of angular momentum unloading (Ismail & Varatharajoo, 2010). The paper develops an attitude control law for the life-support satellite, based on feedback linearization, and tests it by implementing mission controllers based on both Linear Quadratic Regulator (LQR) and Model Predictive Control (MPC), controlling the coupled system composed by the original and the life-support satellites.

It will be shown that the proposed control strategy does not require communication between the life-support system and the satellite, with clear advantages in terms of dedicated interfaces and energy efficiency.

The paper is organized as follows: Section 2 contains a brief review of the state of the art on attitude control related problems and highlights the main paper contributions; Section 3 discusses the preliminary notions necessary to introduce the problem of attitude control; Section 4 introduces the problem of feedback linearization, as it is the theoretical backbone of the

[*] Corresponding author: A. Giuseppi, e-mail: giuseppi@diag.uniroma1.it, phone\fax: 0039-06-77274040.

Conflict of interest - none declared

paper; Section 5 formulates the attitude control problem for the joint satellite and life-support system, highlighting the control scheme for a typical satellite mission and proposing a nested control strategy that utilizes feedback linearization and LQR or MPC; Section 6 shows the results of numerical simulations, based on a real case study, to validate the proposed approach in various operative scenarios; finally, Section 7 draws the conclusions and outlines some future researches.

2 State-of-the-Art Review and Paper Contribution

The problem of attitude control has always been considered one of the most crucial fields of research in space engineering for its relation to satellite operations (Kaplan, 1976). Several types of attitude controllers have been proposed, ranging from sliding-mode ones (Lo & Chen, 1995) to robust PID (Long-Life Show, Jyh-Ching Juang, Chen-Tsung Lin, & Ying-Wen Jan, 2002) and passivity-based ones (Lizarralde & Wen, 1996). In most of the works reported in this review, the satellite has been modeled as a rigid body and, consequently, the differential equations describing the attitude evolution have been derived from basic kinematics and dynamics rules. Starting from a rigid-body model, one of the most used control techniques in satellite attitude control is feedback linearization, as, e.g., in (Bang, Lee, & Eun, 2004a), and (Navabi & Hosseini, 2017). In both papers, the authors consider the satellite system model described in the Byrnes-Isidori *normal form* (Isidori, 1995), derived by the measurement of the so-called "vector components" of the quaternion representation of the satellite attitude (see Section 3).

Several other papers, as (Wie & Barba, 1985) and (Ghiglino, Forshaw, & Lappas, 2015), utilize the quaternion representation to develop their control strategy discussing, respectively, stability related results for large angle maneuvers, derived from Lyapunov's theory, and optimal LQR-based control results. Regarding stability, a significant contribution was given by (Wen & Kreutz-Delgado, 1991), discussing the global properties of several control laws for quaternion represented attitude problems.

The advantages and shortcomings of the quaternion representation have been discussed extensively in (Markley & Crassidis, 2014), (Kaplan, 1976) and (Zipfel, 2007), and such representation is commonly found also in attitude control problem even outside the field of space systems, as in (Fresk & Nikolakopoulos, 2013) and (Reyes-Valeria, Enriquez-Caldera, Camacho-Lara, & Guichard, 2013). In this paper, the so-called *error quaternions* (see Section 5.3) are used, which, for example, were also considered in (Wang, Yuan, & Zhu, 2005) to tackle the earth observation problem by means of a PID control.

Few papers in the literature deal with the operational life extension of a satellite by means of an external support system, and instead typically focus on fault-tolerant control solutions, as (Byrnes & Isidori, 1991; Xiao, Hu, & Zhang, 2012; Zou & Kumar, 2011). In (Byrnes & Isidori, 1991), a smooth state-feedback control is developed to asymptotically stabilize a satellite, whose operation was compromised by a faulty thruster, around the desired attitude. In (Xiao et al., 2012), a sliding mode control is proposed, taking into account the limitation on the maximum torque and momentum of the reaction wheels available on the satellite. In (Zou & Kumar, 2011), the authors presented an adaptive controller based on fuzzy logic and backstepping to obtain robust performances with respect to uncertainties in inertia estimation, actuator faults and external disturbances.

Finally, several moment unloading techniques have been studied in order to desaturate the reaction wheels – that are the main control actuators in most of the works presented so far – using either magnetorquers or thrusters to get the external torque required to perform the task while maintaining the desired attitude, as in (Tregouet, Arzelier, Peaucelle, Pittet, & Zaccarian, 2015) and (Yang, 2017).

With respect to the mentioned literature, the main contributions of this work are the following ones:

- the modelling and control of a two-body satellite system, formed by the composition of the original satellite and a life-support device able to extend its operational life, and the definition of a control scheme able to assure the feedback linearization of the whole system, not relying on information exchanges between the original satellite and the support system;
- the development of a control law, not reliant on information exchanges between the original satellite and the support system, based on feedback linearization, able to assure asymptotic convergence to the desired attitude, even if the actuators of the original satellite are out-of-order;
- the formulation of the attitude tracking problem for the two-body system in terms of LQR and MPC control, by means of error quaternion modelling;
- the integration of a reaction wheel moment unloading control to assure the stability of the system and the feasibility of the control.

3 Preliminaries on Satellite Attitude Control

Quaternions are a convenient way to model the attitude of a rigid body, as they are not affected by singularities such as Euler angles. A unitary quaternion is defined as a 4×1 unitary vector $\boldsymbol{q}$:

$$\boldsymbol{q} = \begin{bmatrix} \boldsymbol{q_{13}} \\ q_4 \end{bmatrix} \in \mathbb{R}^4,$$

where $\boldsymbol{q_{13}} \in \mathbb{R}^3$ takes the name of "vector component" of the quaternion $\boldsymbol{q}$ and $q_4 \in \mathbb{R}$ is its "scalar component".

Some useful operators are defined as follows:

- the cross product between two quaternions $\boldsymbol{q^1}, \boldsymbol{q^2}$, defined as

$$\boldsymbol{q^1} \otimes \boldsymbol{q^2} = \begin{bmatrix} q_4^2 \boldsymbol{q_{13}^1} + q_4^1 \boldsymbol{q_{13}^2} - \boldsymbol{q_{13}^1} \times \boldsymbol{q_{13}^2} \\ q_4^1 q_4^2 - \boldsymbol{q_{13}^1} \cdot \boldsymbol{q_{13}^2} \end{bmatrix}; \tag{1}$$

- the cross product between a (3×1)-vector $\boldsymbol{x}$ and a quaternion $\boldsymbol{q}$

$$\boldsymbol{x} \otimes \boldsymbol{q} = \begin{bmatrix} \boldsymbol{x} \\ 0 \end{bmatrix} \otimes \boldsymbol{q} = [\boldsymbol{x} \otimes]\boldsymbol{q};$$

- the operator

$$[\boldsymbol{q} \otimes] = \begin{bmatrix} q_4 \boldsymbol{I_3} - [\boldsymbol{q_{13}} \times] & \boldsymbol{q_{13}} \\ -\boldsymbol{q_{13}^T} & q_4 \end{bmatrix},$$

where $\boldsymbol{I_n}$ denotes the $(n \times n)$ identity matrix and

$$[\boldsymbol{q} \times] = \begin{bmatrix} 0 & -q_3 & q_2 \\ q_3 & 0 & -q_1 \\ -q_2 & q_1 & 0 \end{bmatrix}; \tag{2}$$

- the operator

$$\Xi(\boldsymbol{q}) = \begin{bmatrix} q_4 \boldsymbol{I_3} + [\boldsymbol{q_{13}} \times] \\ -\boldsymbol{q_{13}^T} \end{bmatrix} = \begin{bmatrix} q_4 & -q_3 & q_2 \\ q_3 & q_4 & -q_1 \\ -q_2 & q_1 & q_4 \\ -q_1 & -q_2 & -q_3 \end{bmatrix}.$$

Finally, the model of the rigid spacecraft with state vector $\boldsymbol{x} = [\boldsymbol{q}\ \boldsymbol{\omega}]^T$ is derived, as customary in the literature (Markley & Crassidis, 2014), as

$$\begin{cases} \dot{\boldsymbol{q}} = \frac{1}{2}\,[\boldsymbol{\omega} \otimes]\boldsymbol{q} \\ \dot{\boldsymbol{\omega}} = \boldsymbol{J_B^{-1}}[\boldsymbol{\tau} - \boldsymbol{\tau_w} - \boldsymbol{\omega} \times (\boldsymbol{J_B}\boldsymbol{\omega} + \boldsymbol{L_w})] \\ \dot{\boldsymbol{L}}_{\boldsymbol{w}} = \boldsymbol{\tau_w} \end{cases} \tag{3}$$

in which: $\boldsymbol{\omega}$ is the angular velocity vector, that represents the rotational velocity of the inertial reference frame with respect to the body frame in the latter coordinates; $\boldsymbol{q}$ is the satellite attitude expressed in quaternions; $\boldsymbol{\tau_w}$ and $\boldsymbol{L_w}$ are the torques applied by the reaction wheels and by their angular momentum, respectively; the disturbance $\boldsymbol{\tau}$ models external forces, including the ones provided by the thrusters of the satellite; $\boldsymbol{J_B}$ is the Moment of Inertia (MOI) tensor, expressed in the rigid body reference frame.

Note that, other than the kinematic equation of $\boldsymbol{q}$, the model (3) includes the dynamical description of $\boldsymbol{\omega}$, which is governed by $\boldsymbol{\tau_w}$ and $\boldsymbol{L_w}$.

4 Preliminaries on Feedback Linearization

In the Multi Input Multi Output (MIMO) case, the problem of feedback linearization consists in finding a control law $\boldsymbol{u}$ such that the nonlinear system

$$\begin{cases} \dot{\boldsymbol{x}} = \boldsymbol{f}(\boldsymbol{x}) + \sum_{i=1}^{m} g_i(\boldsymbol{x}) u_i \\ \boldsymbol{y} = \boldsymbol{h}(\boldsymbol{x}) \end{cases}, \tag{4}$$

with m inputs and c outputs and where

$$\begin{gathered} \boldsymbol{x}(t) = \in \mathbb{R}^n, \\ \boldsymbol{u}(t) = \in \mathbb{R}^m, \\ \boldsymbol{y}(t) = \in \mathbb{R}^c, \\ \boldsymbol{f}(\boldsymbol{x}) = [f_1(\boldsymbol{x}), \dots, f_n(\boldsymbol{x})], \\ \boldsymbol{h}(\boldsymbol{x}) = [h_1(\boldsymbol{x}), \dots, h_c(\boldsymbol{x})], \end{gathered}$$

is reduced, around the origin $\boldsymbol{x_0}$, to a system with a linear input-output map.

For square MIMO systems, the problem of feedback linearization around $\boldsymbol{x_0}$ has a solution if and only if the system has a vector of relative degree $[r_1 \dots r_m]$ in $\boldsymbol{x_0}$, with $\sum_{i=1,\dots,m} r_i \leq n$ (Isidori, 1995) and the decoupling matrix

$$\boldsymbol{\Delta}(\boldsymbol{x}) = \begin{bmatrix} L_{g_1} L_{\boldsymbol{f}}^{r_1 - 1} h_1(\boldsymbol{x}) & \dots & L_{g_m} L_{\boldsymbol{f}}^{r_1 - 1} h_1(\boldsymbol{x}) \\ \vdots & \ddots & \vdots \\ L_{g_1} L_{\boldsymbol{f}}^{r_m - 1} h_m(\boldsymbol{x}) & \dots & L_{g_m} L_{\boldsymbol{f}}^{r_m - 1} h_m(\boldsymbol{x}) \end{bmatrix} \tag{5}$$

is nonsingular in $\boldsymbol{x_0}$.

The control input that realizes the feedback linearization assumes the form

$$\boldsymbol{u} = \boldsymbol{\Delta}(\boldsymbol{x})^{-1}(\boldsymbol{\nu} - \boldsymbol{a}(\boldsymbol{x})), \tag{6}$$

with

$$\boldsymbol{a}(\boldsymbol{x}) = \begin{bmatrix} L_{\boldsymbol{f}}^{r_1} h_1(\boldsymbol{x}) \\ \vdots \\ L_{\boldsymbol{f}}^{r_m} h_m(\boldsymbol{x}) \end{bmatrix} \tag{7}$$

and ν being the control signal that governs the linearized system.

The resulting feedback-linearized system (4) in normal form is then

$$\begin{cases} \dot{\boldsymbol{\xi}} = \boldsymbol{A}\boldsymbol{\xi} + \boldsymbol{B}\boldsymbol{\nu} \\ \dot{\boldsymbol{\eta}} = \boldsymbol{z}(\boldsymbol{\xi}, \boldsymbol{\eta}) \\ \boldsymbol{y} = \boldsymbol{C}\boldsymbol{\xi} \end{cases}, \tag{8}$$

where $\boldsymbol{z}(\boldsymbol{\xi},\boldsymbol{\eta})$ is a smooth function, $\boldsymbol{A} = diag(\boldsymbol{A_1},\boldsymbol{A_2},\boldsymbol{A_3})$, $\boldsymbol{B} = diag(\boldsymbol{B_1},\boldsymbol{B_2},\boldsymbol{B_3})$, and $\boldsymbol{C} = diag(\boldsymbol{C_1},\boldsymbol{C_2},\boldsymbol{C_3})$, are block-diagonal matrices with

$$\boldsymbol{A_i} = \begin{bmatrix} 0 & 1 \\ 0 & 0 \end{bmatrix}, \boldsymbol{B_i} = \begin{bmatrix} 0 \\ 1 \end{bmatrix}, \boldsymbol{C_i} = [0 \quad 1],\ i = 1,2,3.$$

5 Problem Formulation and Control Design

This section presents the feedback-linearized satellite model (section 5.1), the model of the overall satellite and life-support system (section 5.2) and the proposed controller (section 5.3).

5.1 Feedback-Linearized Satellite Model

Following (Bang, Lee, & Eun, 2004b), this paper considers $\boldsymbol{x} = [\boldsymbol{q},\boldsymbol{\omega},\boldsymbol{L_w}]^T$, $\boldsymbol{y} = \boldsymbol{q_{13}}$ and $\boldsymbol{u} = \boldsymbol{\tau_w}$ as state, output and input vectors of the system (3), respectively, and relies on the following assumption for the model:

Assumption 1. In the derivation of the normal form, this paper will consider the model (3), neglecting the dynamics of $\boldsymbol{L_w}$ (i.e., the third equation of (3)), and will assume $\boldsymbol{L_w}$ to be a measured disturbance.

Note that the measure of $\boldsymbol{L_w}$ will be directly utilized (see Section 5.3) to compute dedicated control actions to assure the stability of the dynamics of $\boldsymbol{L_w}$ – separating the problems of moment unloading and attitude control is a standard practice. In alternative to Assumption 1, the dynamics of $\boldsymbol{L_w}$ could be considered as included in the zero dynamics and, as long as its stability is guaranteed by the mentioned dedicated controller, the results of the following sections would still hold. In this work, it was chosen to neglect the dynamics of $\boldsymbol{L_w}$ for the sake of simplicity of the presentation.

With the selected inputs and outputs, the vector of relative degree is $\boldsymbol{r} = [2\ \ 2\ \ 2]^T$ and, assuming, as customary, that the diagonal inertia tensor is $\boldsymbol{J_B} = \mathrm{diag}(I_x, I_y, I_z)$, the decoupling matrix (5) is written as

$$\boldsymbol{\Delta}(\boldsymbol{x}) = -\begin{bmatrix} \frac{q_4}{2I_x} & -\frac{q_3}{2I_y} & \frac{q_2}{2I_z} \\ \frac{q_3}{2I_x} & \frac{q_4}{2I_y} & -\frac{q_1}{2I_z} \\ -\frac{q_2}{2I_x} & \frac{q_1}{2I_y} & \frac{q_4}{2I_z} \end{bmatrix}, \tag{9}$$

whose determinant is

$$\det(\boldsymbol{\Delta}(\boldsymbol{x})) = -q_4 \frac{(q_1^2+q_2^2+q_3^2+q_4^2)}{8I_xI_yI_z}, \tag{10}$$

which annihilates for $q_4 = 0$. It is then possible to feedback-linearize the system via the control (6) for $q_4 \neq 0$, under the following transformation:

$$\begin{bmatrix} \xi \\ \eta \end{bmatrix} = \begin{bmatrix} q_1 \\ \dot{q}_1 \\ q_2 \\ \dot{q}_2 \\ q_3 \\ \dot{q}_3 \\ q_4 \end{bmatrix} = \frac{1}{2}\begin{bmatrix} q_1 \\ (\omega_x q_4 + \omega_z q_2 - \omega_y q_3) \\ q_2 \\ (\omega_y q_4 - \omega_z q_1 + \omega_x q_3) \\ q_3 \\ (\omega_z q_4 + \omega_y q_1 - \omega_x q_2) \\ q_4 \end{bmatrix}, \tag{11}$$

yielding to the normal form (8), from which it follows $\boldsymbol{\ddot{q}_{13}} = \boldsymbol{v}$.

Noting that the unitary properties of the quaternions is preserved over the attitude dynamics, if q_1, q_2 and q_3 converge to appropriate values, q_4, and hence the zero-dynamics, does not diverge.

5.2 Satellite with Support System Model

To control the system formed by the composition of the original satellite with the life-support system, it is needed to model the rigid body representing the overall system and to develop a suitable control scheme that should be deployed into the life-support device.

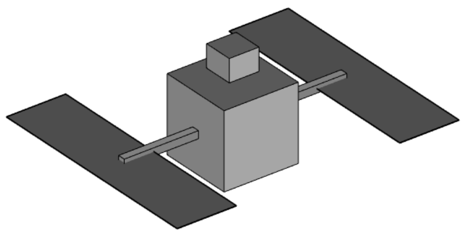

Figure 1 Satellite and Life-Support device connected

The system depicted in Figure 1 is considered, in which:

- the coupling between the life-support device and the satellite is rigid and no joint motion is involved;
- the support system is equipped with reaction wheels for the proper attitude control and with thrusters to perform moment unloading, whereas the satellite may have depleted the propellant and/or have out-of-order actuators;
- the Center Of Mass (COM) of the satellite is aligned with respect to the z-axis of the rigid body reference frame of the support device; the x and y axes of the two reference frames are assumed to be parallel.

The original satellite and the support system are modelled as two cubes with mass m_1 and m_2 and edges of length l_1 and l_2, respectively. Let $m = m_1 + m_2$ and let $\boldsymbol{J^1}$ and $\boldsymbol{J^2}$ be the MOI tensors of the two bodies, expressed in their rigid body reference frames. To characterize the dynamics of the composite system, it is needed to derive its inertia tensor utilizing the Huygens-Steiner – or parallel axis – theorem (Goldstein, Poole, Safko, & Addison, 2002):

$$J_n = J_c + m[(r^T r)I_3 - rr^T], \tag{12}$$

where $\boldsymbol{r}$ is the displacement vector between the COM and the new point where the momentum $\boldsymbol{J_n}$ is calculated, while $\boldsymbol{J_c}$ is the momentum with respect to the COM.

Let z_2 be the z-coordinate of the COM of the support system in the reference frame of the satellite. In the composite body reference frame, the coordinates of the COMs of the two original systems are

$$COM_1 = \begin{bmatrix} 0 \\ 0 \\ -\frac{m_2 z_2}{m} \end{bmatrix}, COM_2 = \begin{bmatrix} 0 \\ 0 \\ \frac{m_1 z_2}{m} \end{bmatrix},$$

respectively. Thanks to (12), the inertia $\boldsymbol{J^2_{COM_1}}$ of the support system evaluated in $\boldsymbol{COM_1}$ is derived as:

$$J^2_{COM_1} = J^2 + m_2 \begin{bmatrix} {z_2}^2 & 0 & 0 \\ 0 & {z_2}^2 & 0 \\ 0 & 0 & 0 \end{bmatrix}.$$

It is now possible to evaluate the inertia tensor $\boldsymbol{J^{Tot}_{COM_1}}$ of the composite body about $\boldsymbol{COM_1}$ as follows:

$$J^{Tot}_{COM_1} = J^1 + J^2_{COM_1}.$$

Finally, the MOI of the composite body in its reference frame is

$$J^{Tot} = J^{Tot}_{COM_1} - m \begin{bmatrix} \left(\frac{m_2 z_2}{m}\right)^2 & 0 & 0 \\ 0 & \left(\frac{m_2 z_2}{m}\right)^2 & 0 \\ 0 & 0 & 0 \end{bmatrix}.$$

Recalling that $z_2 = \frac{l_1}{2} + \frac{l_2}{2}$, it follows:

$$J^{Tot} = J^1 + J^2 + \begin{bmatrix} m_2\left(\frac{l_1+l_2}{2}\right)^2 & 0 & 0 \\ 0 & m_2\left(\frac{l_1+l_2}{2}\right)^2 & 0 \\ 0 & 0 & 0 \end{bmatrix} + \\ - \begin{bmatrix} \frac{{m_2}^2(l_1+l_2)^2}{4m} & 0 & 0 \\ 0 & \frac{{m_2}^2(l_1+l_2)^2}{4m} & 0 \\ 0 & 0 & 0 \end{bmatrix}. \tag{13}$$

The system dynamics is then unchanged, save for the new value of the MOI and the presence of new reaction wheels, whose angular momentum, $\boldsymbol{L_{wn}}$, follows $\dot{\boldsymbol{L}}_{\mathbf{wn}} = \boldsymbol{\tau_{wn}}$.

5.3 Proposed Controllers

Overall Control System

Figure 2 reports a typical scheme for the satellite attitude control problem, applied to the composite system. An outer control loop, governed by a mission controller, is responsible for the tracking of the reference attitude trajectory, while an internal control loop is responsible for the feedback linearization – which simplifies the task of the mission controller. An additional controller is in charge of managing the momentum built up into the reaction wheels, typically by unloading it according to heuristic laws to avoid their saturation.

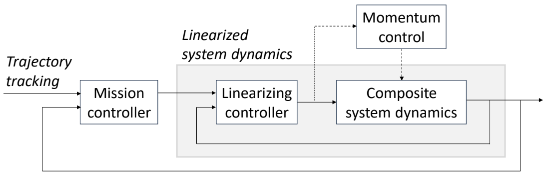

Figure 2 Satellite attitude control via feedback linearization

The following subsections are going to detail each one of the proposed controllers.

Feedback Linearization of the composite system

It is assumed that the original satellite is controlled by a scheme analogous to the one reported in Figure 2, i.e., the satellite is already equipped with a feedback-linearizing controller, which, at the time of the connection, is still active. After the attachment, it follows that

$$\ddot{q}_{13} = a(q, L_w + L_{wn}, \omega, J^{Tot}) + \Delta(J^{tot}, q)u,$$

where $\boldsymbol{a}(\cdot)$ and $\boldsymbol{\Delta}(\cdot)$ are, with a slight abuse of notation, as in (7), (9).

To apply feedback linearization, the required input of the overall system, $\boldsymbol{u_{req}}$, would have to be set to

$$u_{req} = \Delta(J^{Tot}, q)^{-1}[v - a(q, L_w + L_{wn}, \omega, J^{Tot})], \tag{14}$$

but this control law does not consider that the original satellite is already applying, unaware of the presence of the life-support device, its feedback linearization law:

$$u_1 = \Delta(J^1, q)^{-1}[v - a(q, L_w, \omega, J^1)]. \tag{15}$$

In order to provide a solution for the support of an operative satellite (e.g., in a mission that desires to update the scientific instruments of the satellite), one may think of cancelling the original linearizing controller, actuated by the sole satellite, and of substituting it with a new linearizing controller for the overall system, as depicted in Figure 3.

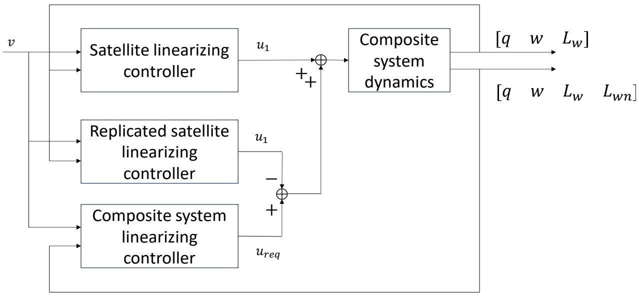

Figure 3 Feedback-linearizing controller

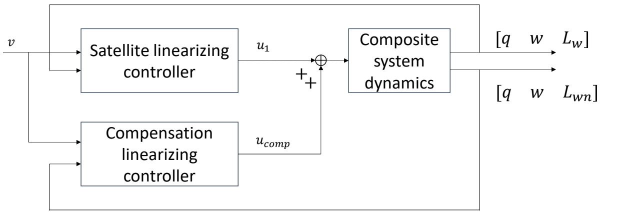

Figure 4. Feedback-linearizing compensation controller

This approach trivially requires the support device to compute a replica of $\boldsymbol{u_1}$ and subtract it from $\boldsymbol{u_{req}}$ before applying it to the system. With this solution, besides the mission control command $\boldsymbol{v}$, the support system needs the sensor readings regarding $\boldsymbol{q}$, $\boldsymbol{\omega}$ and $\boldsymbol{L_w}$. Even if the former two signals, $\boldsymbol{q}$ and $\boldsymbol{\omega}$, are the same for the satellite and the support system, there is still the signal $\boldsymbol{L_w}$ that must be communicated by the satellite to the support system. This need of communication affects the feasibility of the proposed scheme for all the satellites which are not already provided with an appropriate communication channel.

To overcome this problem, it will be shown in the following that it is possible to design a *compensation* controller which directly computes an additive control action that compensates the presence of $\boldsymbol{u_1}$ without having to explicitly compute $\boldsymbol{u_1}$ on-line. In other words, to obtain the objective of not interfering with the control logic of the original satellite, the controller compensates the linearizing control $\boldsymbol{u_1}$ with an additional action $\boldsymbol{u_{comp}}$ in such a way that $\boldsymbol{u_{req}}$ is recovered as $\boldsymbol{u_{req}} = \boldsymbol{u_1} + \boldsymbol{u_{comp}}$ (see Figure 4). It will also be shown that the compensation control action will not require the measures of $\boldsymbol{L_w}$.

Let us consider the control scheme of Figure 4 and let the feedback-linearizing compensation torque be

$$\boldsymbol{u_{comp}} = \boldsymbol{u_{req}} - \boldsymbol{u_1}, \tag{16}$$

which, substituting (14) and (15), becomes:

$$\boldsymbol{u_{comp}} = \boldsymbol{\Delta}\left(\boldsymbol{J^{Tot}}, \boldsymbol{q}\right)^{-1}\left[-\boldsymbol{a}(\boldsymbol{q}, \boldsymbol{L_w} + \boldsymbol{L_{wn}}, \boldsymbol{\omega}, \boldsymbol{J^{Tot}}\right] + \\ -\boldsymbol{\Delta}\left(\boldsymbol{J^1}, \boldsymbol{q}\right)^{-1}\left[\boldsymbol{v} - \boldsymbol{a}\left(\boldsymbol{q}, \boldsymbol{L_w}, \boldsymbol{\omega}, \boldsymbol{J^1}\right)\right]. \tag{17}$$

Considering the model (3), with reaction wheels and without external forces applied, setting

$$\boldsymbol{\tau_w} = -\boldsymbol{J^1}\widetilde{\boldsymbol{u}} - \boldsymbol{\omega} \times (\boldsymbol{J^1}\boldsymbol{\omega} + \boldsymbol{L_w}),$$

in which $\widetilde{\boldsymbol{u}}$ is a *proxy control* introduced in the following analysis, it follows $\dot{\boldsymbol{\omega}} = \widetilde{\boldsymbol{u}}$.

By defining $\boldsymbol{Q}(\boldsymbol{q})$ as the vector including the first three rows of the matrix $\frac{1}{2}\boldsymbol{\Xi}(\boldsymbol{q})$, one has that

$$\ddot{\boldsymbol{q}}_{\boldsymbol{13}} = \mathbf{Q}(\boldsymbol{q})\,\dot{\boldsymbol{\omega}} + \mathbf{Q}(\dot{\boldsymbol{q}})\,\boldsymbol{\omega},$$

Therefore, by setting

$$\widetilde{\boldsymbol{u}} = \dot{\boldsymbol{\omega}} = \boldsymbol{Q}(\boldsymbol{q})^{-1}(\boldsymbol{v} - \boldsymbol{Q}(\dot{\boldsymbol{q}})\boldsymbol{\omega}),$$

the feedback linearized system $\ddot{\boldsymbol{q}}_{\boldsymbol{13}} = \boldsymbol{v}$ is recovered.

The feedback linearization torque is then

$$\boldsymbol{u_1} = \boldsymbol{t_w} = \\ = -\boldsymbol{J^1}\boldsymbol{Q}(\boldsymbol{q})^{-1}(\boldsymbol{v} - \boldsymbol{Q}(\dot{\boldsymbol{q}})\boldsymbol{\omega}) - \boldsymbol{\omega} \times \left(\boldsymbol{J^1}\boldsymbol{\omega} + \boldsymbol{L_w}\right). \tag{18}$$

Substituting (18) and (14) into (16) gives us the final expression for the feedback-linearizing compensation torque:

$$\boldsymbol{u_{comp}} = -\left(\boldsymbol{J^{tot}} - \boldsymbol{J^1}\right)\boldsymbol{Q}(\boldsymbol{q})^{-1}[\boldsymbol{v} - \boldsymbol{Q}(\dot{\boldsymbol{q}})\boldsymbol{\omega}] - \boldsymbol{\omega} \times \\ \left[\left(\boldsymbol{J^{tot}} - \boldsymbol{J^1}\right)\boldsymbol{\omega} + \boldsymbol{L_{wn}}\right], \tag{19}$$

which has the same expression of $\boldsymbol{u_1}$ in equation (18), with $\left(\boldsymbol{J^{tot}} - \boldsymbol{J^1}\right)$ as inertia term and $\boldsymbol{L_{wn}}$ as the momentum of the wheels.

Remark 2. The control law (19) does not depend on $\boldsymbol{L_w}$: the support system does not require information regarding the momentum of the reaction wheels of the original satellite, and the only exogeneous signal it receives is $\boldsymbol{v}$, which could even be obtained directly by the measurements of $\boldsymbol{q}$ if the support is equipped with a replica of the outer loop controller. This independence is one of the most significant advantages of the proposed control scheme of Figure 4, as it does not require any communication interfaces between the two systems and can hence be deployed to satellites already in orbit. As a by-product, the communication-less control scheme is valuable also from the energy-saving viewpoint.

Remark 3. The control law (19) considers that the satellite is still operating its reaction wheels, and, thus, its dynamics is already feedback-linearized. In this scenario, the support is needed, e.g., to provide new thrusters or scientific equipment. In case the life-support system has been attached to a satellite that can no longer operate its reaction wheels, the support system oversees the whole control actuation, including the feedback linearization of the complete system. To this end, if the reaction wheels of the satellite are no longer operative, the support system has to directly apply the control law (14) with null $\boldsymbol{L_w}$.

Mission Controller

This section analyses the design of the outer loop controller, which operates on the linearized composite satellite system and whose task is to let the system track a reference trajectory. It is worth remarking that the proposed control scheme is, in general, independent of the implemented mission controller. In fact, any control law designed for a feedback linearized satellite is compatible with the proposed scheme, as the life-support compensates its effect on the system dynamics by providing an additional control action.

To apply standard tracking control algorithms for linear systems, a change of the coordinates of the system (8) is needed, as the typical satellite mission does not require to drive the system to its origin but, instead, requires the tracking of a reference trajectory $\boldsymbol{q^{ref}}(t)$. A trivial solution for the tracking problem would then be the annihilation of the error $\boldsymbol{e}(t) = \boldsymbol{q_{13}^{ref}}(t) - \boldsymbol{q_{13}}(t)$, which, under feedback linearization (14), would lead to

$$\ddot{\boldsymbol{e}}(t) = \ddot{\boldsymbol{q}}_{\boldsymbol{13}}^{\boldsymbol{ref}}(t) - \boldsymbol{\nu}(t) = \tilde{\boldsymbol{\nu}}(t),$$

where $\tilde{\boldsymbol{\nu}}(t)$ is a *proxy control* that governs the error dynamics. The limit of this approach is that the system has no control over the convergence value of q_4, meaning that, without proper considerations, the satellite may attain an attitude that is different from the desired one.

It is then convenient to write the system in the so-called error quaternions coordinates (Markley & Crassidis, 2014; Wang et al., 2005), defined as

$$\boldsymbol{\delta} = \begin{bmatrix} \boldsymbol{\delta_{13}} \\ \delta_4 \end{bmatrix} = \boldsymbol{q} \otimes \boldsymbol{q^0}^{-1},$$

where $\boldsymbol{q^0}^{-1}$ is the inverse o the quaternion $\boldsymbol{q^0}$, yielding

$$\boldsymbol{\delta_{13}} = \Xi(\boldsymbol{q^0})\boldsymbol{q},$$
$$\delta_4 = \boldsymbol{q^0}^{\mathrm{T}}\boldsymbol{q}.$$

The error quaternion represents the rotational error between the quaternion $\boldsymbol{q}$ and an arbitrary quaternion $\boldsymbol{q^0}$. By choosing a reference trajectory in the error quaternion coordinates $\boldsymbol{\delta_{13}^{ref}}(t)$ that converges to $[0\ 0\ 0]^T$ (i.e., $\boldsymbol{q^{ref}}(t) \to \boldsymbol{q^0}$), the tracking error is defined as

$$\boldsymbol{\delta_e}(\mathrm{t}) = \boldsymbol{\delta_{13}}(\mathrm{t}) - \boldsymbol{\delta_{13}^{ref}}(\mathrm{t}). \quad (20)$$

Due to the particular choice of $\boldsymbol{q^0}$, annihilating this error asymptotically drives the system to either the identity quaternion $\boldsymbol{I} = [0,0,0,1]^T$ or to $-\boldsymbol{I}$, which represent the same attitude, avoiding then the ambiguity of a formulation based on the error $\boldsymbol{e}$. For a fixed $\boldsymbol{q^0}$, the dynamics of the system becomes

$$\dot{\boldsymbol{\delta}} = \dot{\boldsymbol{q}} \otimes \boldsymbol{q^0}^{-1} = \frac{1}{2}[\boldsymbol{\omega}(t) \otimes]\boldsymbol{q}(t) \otimes \boldsymbol{q^0}^{-1} = \frac{1}{2}[\boldsymbol{\omega}(t) \otimes]\boldsymbol{\delta}, \quad (21)$$

i.e., the dynamics (21) of the system in the error quaternion coordinates is the same as in the original coordinates.

Remark 4. Considering that the dynamics of $\boldsymbol{\delta}$ and $\boldsymbol{q}$ are the same, all the results of Section 5.1 and Section 5.3 still hold with a trivial coordinate substitution. In particular, the feedback linearization feasibility condition, derived from the nonsingularity of (9), translates to $\delta_4(t) \neq 0$. The boundness of $\delta_4(t)$, yields that any controller that annihilates $\boldsymbol{\delta_e}$ stabilizes the two-body systems and achieves tracking.

Mission Controller based on Linear Quadratic Regulator (LQR)

The LQR is one of the most used controllers for linear systems and relies on the definition of a quadratic cost function that summarizes the control objectives and that usually takes the form:

$$J = \frac{1}{2}\int_{t_0}^{\infty}\left[\boldsymbol{\delta_e}^T\boldsymbol{Q}(t)\boldsymbol{\delta_e} + \tilde{\boldsymbol{\nu}}^T\boldsymbol{R}(t)\tilde{\boldsymbol{\nu}}\right]dt, \quad (22)$$

where $\boldsymbol{Q}(t)$ and $\boldsymbol{R}(t)$ are positively definite matrices, representing, respectively, the weights assigned to the error values and to the control effort.

In the standard LQR approach (Zhou, Doyle, & Glover, 1996), the control action minimizing (22) is available in closed-form:

$$\tilde{\boldsymbol{\nu}} = -\boldsymbol{R}^{-1}\boldsymbol{B}^T\boldsymbol{K}\boldsymbol{\delta_e}, \quad (23)$$

where $\boldsymbol{K}$ is the solution of the Riccati equation associated with the LQR problem.

The control action to implement in (15) is then:

$$\boldsymbol{\nu} = \ddot{\boldsymbol{\delta}}_{\boldsymbol{13}}^{\boldsymbol{ref}} + \boldsymbol{R}^{-1}\boldsymbol{B}^T\boldsymbol{K}\boldsymbol{\delta_e}. \quad (24)$$

The main limitation of LQR is that the optimization does not take into account the physical limitations of the system or any form of additional constraint. In particular, the LQR formulation cannot guarantee the feedback linearizing condition $\delta_4 \neq 0$ at all times, nor the actuation of the control. A good candidate to address this limitation is then MPC, as described below.

Mission Controller based on Model Predictive Control

The underlying idea of classical MPC is to use a discretized dynamic model of the system, obtained by an exact state-space discretization of the linearized system (8), to predict the state trajectory under a given control action and optimize the system evolution over the so-called *prediction horizon* of length P. The optimization is performed every s seconds and computes the control actions over the period P; subsequently, only the first control action is applied to the system, while the other computed ones are discarded.

With a little abuse of notation, let $\boldsymbol{v}[k|h]$ denote the predicted control action value at time $(h+k)s$ computed at time hs (note that the same notation will be used hereinafter for other signals), and let the optimal control sequence be denoted by $\boldsymbol{v}^*$. The proposed MPC formulation, which is explained in the remainder of the section, is the following:

$$\min_{\boldsymbol{v}\in\mathbb{R}^C} J(\boldsymbol{v}) \tag{25}$$

s.t.

$$\frac{T}{2}(\boldsymbol{\omega}[k|h]^T\boldsymbol{\delta_{13}}[k|h]) - \delta_4[k|h] \le 0, \text{if } \delta_4[k|h] > 0,$$
$$k = 1, \dots, P, \tag{26}$$

$$\frac{T}{2}(\boldsymbol{\omega}[k|h]^T\boldsymbol{\delta_{13}}[k|h]) - \delta_4[k|h] \ge 0, \text{if } \delta_4[k|h] < 0,$$
$$k = 1, \dots, P, \tag{27}$$

$$\boldsymbol{a}(\boldsymbol{x}[k|h]) + \boldsymbol{\Delta}(\boldsymbol{x}[k|h])\boldsymbol{u_{min}} < \boldsymbol{v}[k|h] < \boldsymbol{a}(\boldsymbol{x}[k|h]) + \boldsymbol{\Delta}(\boldsymbol{x}[k|h])\boldsymbol{u_{max}},\ k = 0, \dots, P-1. \tag{28}$$

The cost function (25) has the same rationale of the cost function (22) and is of the form

$$J(\boldsymbol{v}) = \frac{1}{2}\sum_{k=1,\dots,P}(\boldsymbol{\delta_e}[k|h]^T\boldsymbol{Q}[k]\boldsymbol{\delta_e}[k|h] + \boldsymbol{v}[k-1|h]^T\boldsymbol{R}[k-1]\boldsymbol{v}[k-1|h]). \tag{29}$$

MPC provides a framework in which one can directly impose the constraint $\delta_4 \neq 0$ over the prediction window, driving the system to the desired attitude while avoiding the singularity points. In other words, MPC forces the system to follow safer, even if potentially sub-optimal, trajectories.

Note that the feasible solutions are the ones which keep the feedback linearization always active, that is the constraint $\delta_4(t) \neq 0$ must be met for all times $t \in [hT, (h+P)s)$ and not only for the instants $(h+k)s$, $k = 1, \dots, P$. A simple solution is to limit the evolution of δ_4 by constraining its discretized dynamics in a conservative way. From (3), it follows that

$$\delta_4[k+1|h] - \delta_4[k|h] - \frac{T}{2}(\boldsymbol{\omega}[k|h]^T\boldsymbol{\delta_{13}}[k|h]),$$

for $k = 1, \dots, P$, meaning that the constraints (26), (27) guarantee that, in the interval $[ks, (k+1)s)$, δ_4 does not reach the value 0, independently from its sign at time k. In other words, constraints (26), (27) constitute the conditions for the feasibility of the feedback linearization.

Finally, the controller needs to guarantee also that the actuation is feasible, i.e., that the control action computed by the MPC does not saturate the reaction wheels, which, with little abuse of notation, translates into the set of component-wise constraints:

$$\boldsymbol{u_{min}} < \boldsymbol{u}(t) < \boldsymbol{u_{max}}.$$

A possible solution is to properly constrain the available control dedicated to the MPC, depending on the current effort demanded by the feedback linearizing control. From equation (6), it follows that the portion of the control available to the mission control $\boldsymbol{v}$ is then

$$\boldsymbol{a}(\boldsymbol{x}) + \boldsymbol{\Delta}(\boldsymbol{x})\boldsymbol{u_{min}} < \boldsymbol{v} < \boldsymbol{a}(\boldsymbol{x}) + \boldsymbol{\Delta}(\boldsymbol{x})\boldsymbol{u_{max}},$$

which translates into the set (28) of constraints for the MPC controller. In constraints (28), the predicted state $\boldsymbol{x}[k|h]$ is firstly computed in the coordinates $(\boldsymbol{\xi}, \eta)$ by using the candidate control sequence $\boldsymbol{v}$ as input to the discretized version of system (8); then, the predicted state $\boldsymbol{x}[k|h]$ in the original coordinates of (3) (i.e., $(\boldsymbol{q}, \boldsymbol{w}, \boldsymbol{L_w})$) is retrieved using the inverse of the coordinate transformation (11) (which always exists since (11) is a diffeomorphism (Isidori, 1995)).

For the sake of computational complexity reduction, the concept of control horizon is used: starting from time $C \le P$, the controller holds the value $\boldsymbol{v}(C)$ for all the remaining controls $\boldsymbol{v}[C+1|h], \dots, \boldsymbol{v}[P-1|h]$ in the prediction window. Note that this simplification provides a sub-optimal solution, whose quality depends on the length of C.

Momentum Unloading

The problem of momentum unloading is commonly considered as disjoint from the attitude control. To add a momentum control, the dynamical equation of the angular momentum is modified to

$$\dot{\boldsymbol{L_w}} = \boldsymbol{\tau_w} + \boldsymbol{\tau^u},$$

which is stabilized by the simple control law of the form

$$\boldsymbol{\tau_w} + \boldsymbol{\tau^u} = -K\boldsymbol{L^w}, K > 0 \tag{30}$$

One could choose to apply this type of control either during the periods in which no changes in attitude are envisaged and when momentum wheels are close to their saturation, or continuously during the system operation. Following the latter approach, it is possible to set

$$K = \frac{\tau_{max}}{L_w^{sat}},$$

in which τ_{max} represents the maximum torque that the wheels are able to provide and L_w^{sat} is the saturation value of the angular momentum of the wheels. This choice of K entails that the discharge increases when the momentum is close to its saturation and does not significantly affect the system otherwise.

The control law (30) implies that $\boldsymbol{u}$ (recall that $\boldsymbol{u} = \boldsymbol{t_w}$) is conservatively bounded with respect to its nominal values, as the unloading torque absorbs a portion of the available effort. This physical limitation can be implemented as an additional constraint for the MPC controller, with some awareness, by adapting the values of $\boldsymbol{u_{min}}$ and $\boldsymbol{u_{max}}$ in (28) depending on the measured $\boldsymbol{L_w}$. It is worth noting that the receding horizon procedure allows the controller to activate the unloading procedure arbitrarily (e.g., when $\boldsymbol{L_w}$ exceeds a safety threshold) by adding the relative constraints in the optimization. Furthermore, note that to have the unloading torque decoupled from the attitude dynamics, the available thrusters must provide an external torque $\boldsymbol{\tau}$ opposite to $\boldsymbol{\tau^u}$, so that when (30) is applied into the second equation of (3) the original torque $\boldsymbol{\tau_w}$ is recovered.

6 Simulations

Satellite Setup

A medium size GEO telecommunication (TLC) satellite, 16 kW–2500 kg class, has been selected as a reference case to perform the simulation analyses. The life-support vehicle design has been based on a study case of Thales Alenia Space Italia and it has been modelled connected to the customer TLC satellite on its $-z$ "separation" plane. Table 1 reports the main inertia for both the stand-alone satellite and the composed stack configurations. In the first two simulations, the satellite is still operative, and the life-support system is needed to provide new equipment, whereas in the third simulation the satellite has deactivated its actuators and the life-support system is needed to prolong its operation. A fourth simulation assesses the performances of the proposed controller in scenarios characterized by external disturbances, parametric uncertainties and measurement noise. The fifth and final simulation reports a comparative simulation that shows how the proposed scheme can be adapted to scenarios in which the two spacecraft communicate and implements a fault-tolerant control law to renders a satellite with severe faults operative again.

All the following simulations have been implemented in MATLAB® and Simulink®, using their MPC toolbox when relevant.

Table 1 Parameters for the satellite model

Parameter	Value
I_x^1	$20000\ Kg \cdot m^2$
I_y^1	$3000\ Kg \cdot m^2$
I_z^1	$17000\ Kg \cdot m^2$
I_x^{tot}	$34595\ Kg \cdot m^2$
I_y^{tot}	$5695\ Kg \cdot m^2$
I_z^{tot}	$28900\ Kg \cdot m^2$

LQR-based Mission Controller

In the following, an attitude tracking mission is proposed, within the scenario characterized by the quantities reported in Table 2.

Table 2 Parameters for LQR simulations

Parameter	Value
$\delta_1(0)$	0.5109
$\delta_2(0)$	0.32
$\delta_3(0)$	0.1411
T	1500s
$\boldsymbol{Q}$	$\boldsymbol{I_6}$
$\boldsymbol{R}$	$10^9 \cdot \boldsymbol{I_3}$
K	0.03

The reference trajectory for the mission was chosen as follows

$$\boldsymbol{\delta_{13}^{ref}} = \boldsymbol{\delta}(0)e^{-\frac{t}{T}}, \quad (31)$$

i.e., the control should not only let the satellite converge to the reference attitude (that is, in the error quaternion representation, to $\boldsymbol{\delta_{13}} = [0\ 0\ 0]^T$) but, for the success of the mission, it should approach that attitude with an exponential behavior. The time constant T of (31) was set to a value which is realistic for the mission considered in the case study, which requires the control of a TLC satellite that points at a limited area of the earth while orbiting. The complete mission is planned over 10^4 seconds.

Figure 5 shows that the implemented control successfully drives the error quaternion to the identity, i.e., the desired final attitude is reached. Figure 6 reports how the satellite tracks the desired attitude trajectory, highlighting that, after about 1300s, the error annihilates. Figure 7 and Figure 8 report the profiles of the attitude control torques for the original satellite and the support system, respectively, highlighting their shared mathematical structure, in line with the compensator nature of (19). Finally,

Figure 9 reports that the moment unloading law proposed achieves its objective.

Due to the fact that LQR does not guarantee the control feasibility, the weighting matrix $\boldsymbol{R}$ in (22) was set to a high value ($10^9 \cdot \boldsymbol{I_3}$) to reduce the peak values of the control torques to approximately the typical physical limitations of reaction wheels ($\sim 0.1 Nm$).

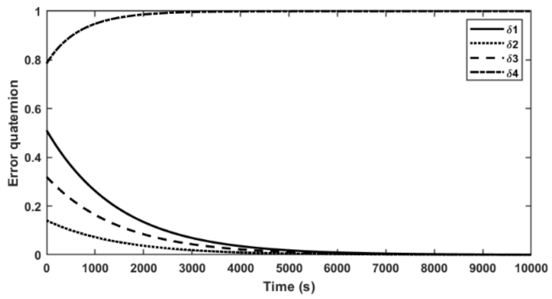

Figure 5 Attitude evolution of satellite's attitude, LQR case

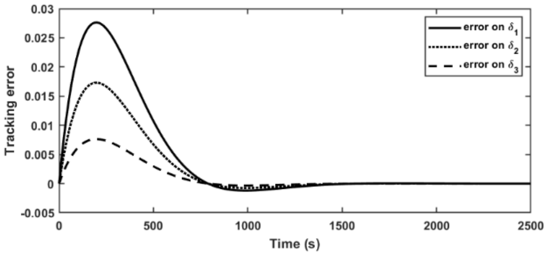

Figure 6 Tracking error evolution, LQR case

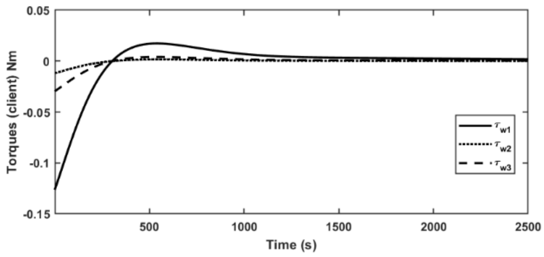

Figure 7 Satellite torque profiles, LQR case

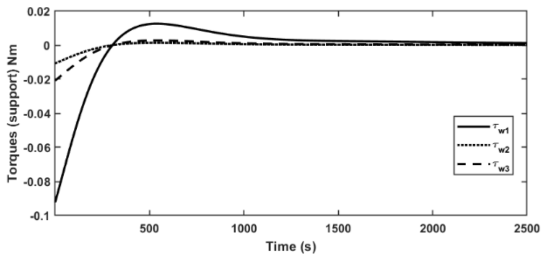

Figure 8 Support torque profiles, LQR case

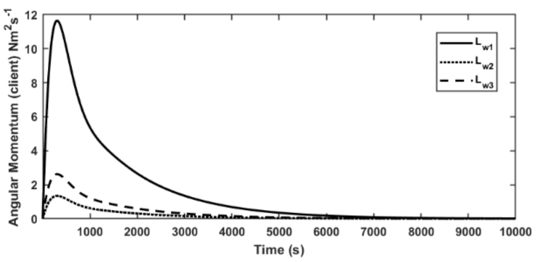

Figure 9 Momentum of the wheels of the Satellite, LQR case

Even with the selected value, Figure 6 shows that the requested control torques are not always within their feasibility margins. To successfully apply the LQR control scheme, during the mission design the control center should consider the expected peak values of the control torques, hence requiring an off-line tuning that may be computationally demanding for missions in which the reference trajectory evolves rapidly.

MPC-based mission controller

The simulation setup is similar to the one of the previous case, with the differences reported in Table 3. The sampling time s for the controller was set to 60s.

Table 3 Parameters for MPC simulations

Parameter	Value
P	100
C	80
$\boldsymbol{Q}$	$\boldsymbol{I_{6\times P}}$
$\boldsymbol{R}$	$10^{-3} \cdot \boldsymbol{I_{3\times P}}$

By taking into account the input saturation directly into the problem formulation (25)-(28), the MPC controller is able to drive the attitude tracking error to zero significantly faster, as reported in Figure 10, since and the saturations do not cause the system to evolve in an unexpected way. Thanks to the assured feasibility of the control torques, the weighting matrix $\boldsymbol{R}$ in (29) can be set to an arbitrarily small diagonal positive definite matrix, allowing the controller to focus on the error annihilation and obtain lower convergence times.

A similar torque behavior is obtained, as before, for both the original satellite and the support system, so is reported only the one of the satellite in Figure 11.

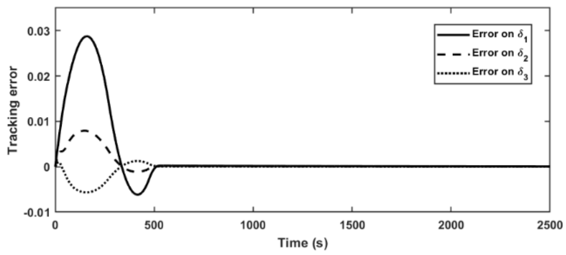

Figure 10 Tracking error evolution, MPC case

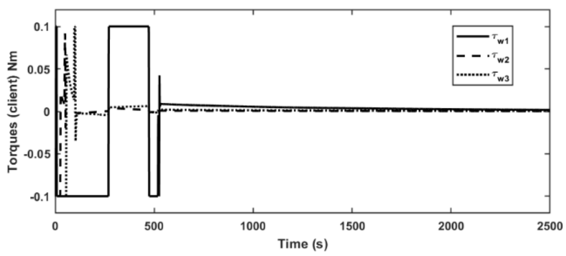

Figure 11 Torque profile for the satellite, MPC case

Since the MPC assures the feasibility of the control by means of singularity avoidance, as explained in

Section 5.3, the MPC controller is preferable overall not only in terms of performances and also flexibility.

MPC mission controller in absence of original satellite control

This simulation considers a scenario in which the original satellite cannot operate its reaction wheels any longer, and hence all the control torques are applied by the life-support device. In this case, the support device enforces the feedback linearizing action of equation (14) instead of the compensating control of equation (19) (see Remark 3).

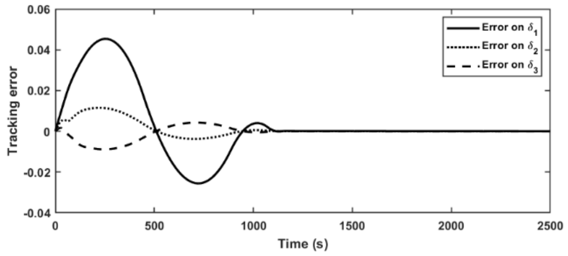

Figure 12 Tracking error evolution, MPC case with non-operative reaction wheels on the satellite

Figure 12 reports the simulation results considering the same scenario of the second simulation and shows that, even if tracking performances have worsened with respect to the previous case, the system is still able to converge to the desired attitude trajectory, successfully making an out-of-order satellite operational again, and still achieving superior performances with respect to the LQR applied to an operative satellite (see the first simulation results).

MPC mission controller in presence of external disturbances, parametric uncertainties and Gaussian white noises

So far, it was assumed that the controller was provided with exact state feedback, but in order to validate the proposed control scheme in a more representative scenario, this assumption may not be reasonable. In fact, even if both the satellite and the life-support are equipped with high-grade star trackers and gyroscopes, respectively for attitude and angular velocity measurements, the measurement noise that affects such sensors cannot be, in principle, neglected. Furthermore, in the previous simulations the MPC controller was provided with an exact evaluation of the MOIs, and no external disturbance was considered.

In this simulation, those simplifications are removed, and, for the sake of comparison, it is assumed that the mission controller is still based on MPC, with the difference that its state feedback is provided by the state estimation obtained from an extended Kalman Filter. It is assumed that the sensors are subject to measurement white Gaussian noises, on attitude and velocity measurements, of zero mean and variances of 10^{-8} and $10^{-6}\, rad/sec$ respectively, in line with (Mehra, Seereeram, Bayard, & Hadaegh, 2002). For the sake of simplicity, the process noise is also assumed to be characterized by the same variances.

The unmeasured and time-varying external disturbances are described by the torque vector

$$\boldsymbol{\tau} = \begin{bmatrix} 0.03\sin(0.01t) \\ 0.02\sin(0.03t) \\ 0.025\sin(0.001t) \end{bmatrix}.$$

Finally, the real MOI components of the two-body system are assumed to be 10% higher than the one provided to the controller and reported in Table 1.

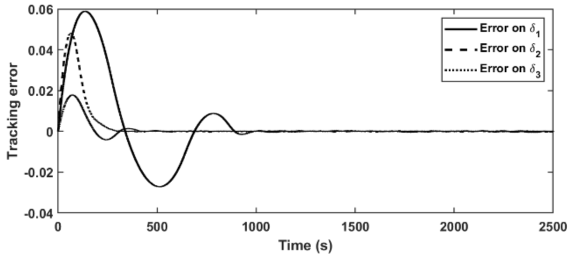

Figure 13 Tracking error evolution, MPC in a realistic scenario

From the analysis of Figure 13, it is evident that the control performances degrade significantly, in both error amplitude and convergence time, but, considering that the controller was mainly designed for a nominal situation, its performances remain reasonable and the attitude tracking mission is still successfully completed.

Using the life-support system to control the satellite in presence of communication

For comparison purposes, this simulation discusses an alternative usage of the life-support system. In this mission, the life-support is used to take over the original satellite control logic and can directly operate the actuators of the satellite. This scenario requires real-time communication between the two systems to exchange measures and control commands, but enables the life-support to implement, in principle, any control logic developed for the problem of attitude tracking. For the sake of comparison, it is further assumed that faults of the actuators are unknown to both controllers, as with the proposed control scheme, and, therefore, a fault-tolerant scheme is considered.

The domain of fault-tolerant control is a natural application of the life-support system: it is an industry standard to provide any satellite with at least four actuators, in order to preserve its operability even in presence of failures, and the life-support, in fact, delivers additional actuators to the orbiting satellite. To this end, the tested control law was derived from the one presented in (Jin, Ko, & Ryoo, 2008), based on Dynamic Inversion and Time-Delay Control.

For this simulation it is assumed that both the satellite and the life-support system are equipped with four reaction wheels. The nominal distribution matrix, that projects the torques provided by the reaction wheels over the principal axes of inertia, is assumed to be, for the two body-system, as follows:

$$\boldsymbol{L_\tau} = \begin{bmatrix} 1 & 1 & -1 & -1 & 1 & 1 & -1 & -1 \\ -1 & 1 & 1 & -1 & -1 & 1 & 1 & -1 \\ \sqrt{2} & \sqrt{2} & \sqrt{2} & \sqrt{2} & \sqrt{2} & \sqrt{2} & \sqrt{2} & \sqrt{2} \end{bmatrix},$$

in which the first four columns are relative to the original satellite actuators, as in (Jin, Ko, & Ryoo, 2008), while the other ones are relative to the life-support system. The distribution of the actuation torques follows $\boldsymbol{\tau_w} = \boldsymbol{L_\tau}\,\boldsymbol{u^{ft}}$, where the fault-tolerant control law $\boldsymbol{u^{ft}}$ is the vector containing the torques commanded to the actuators.

Furthermore, the original satellite presents total faults on the first two of its actuators, so that the satellite system alone would fail to actuate the commanded torques: in fact, such faults translate into having the first two columns of the original 4×4 distribution matrix substituted by zeros, causing its rank to be less than three and, consequently, the satellite is no longer able to attain arbitrary attitudes, even if controlled by fault-tolerant laws. Conversely, in the considered simulation set up, the distribution matrix of the two-body system remains of full rank and the law designed in (Jin, Ko, & Ryoo, 2008) is able to complete the attitude tracking mission.

The two-body spacecraft parameters were the ones reported in Table 1, as in the previous simulations. The reader is referred to (Jin, Ko, & Ryoo, 2008) for details on the control law, which is characterized by the control gains τ_1 and τ_1, set to $\tau_1 = 150$, $\tau_2 = 135$ to account for the considered spacecraft model.

Figure 14 shows the attitude tracking error evolution[1] and Figure 15 presents the actuated control torques. Note that, due to their alignment, the actuation profiles of the remaining reaction wheels of the original satellite coincide with the corresponding ones of the life-support system and are not visible in the figure. It is clear from the figures that the performances have significantly worsened, in particular in terms of error magnitude, but this was expected as the controller calculated the commanded actuation torques having knowledge only on the nominal distribution matrix.

7 Conclusions

This paper presented a control strategy to govern a life-support system that may be attached to a satellite to increase its operational lifespan. The proposed control scheme for the attitude control problem in the presence of such support system consists of two controllers: the inner one is devoted to feedback linearizing the system, whereas the outer controller, which consequently operates on a linear system, oversees the attitude tracking. Two outer controllers were proposed, based on LQR and on MPC. Thanks to the developed control strategy, the life-support device is capable of performing the attitude control task for the two-body system also in case of non-operational actuators of the original satellites, without requiring communication exchange with the original satellite.

Numerical simulations based on a real case study were reported to validate the results presented, in scenarios spacing from ideal to adverse situations.

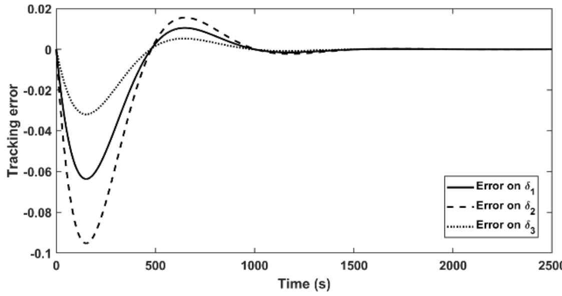

Figure 14 Tracking error evolution, fault-tolerant law

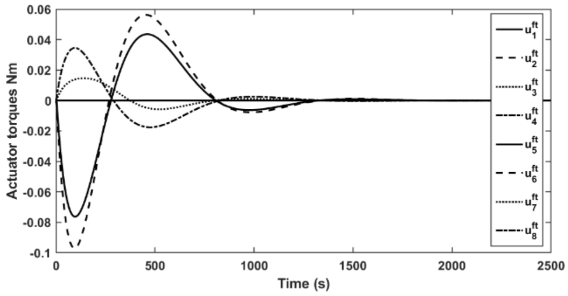

Figure 15 Control torques, fault-tolerant law

Future work is aimed at explicitly providing robustness to the overall scheme, to tackle model inaccuracies, model parameter variations (e.g., due to fuel consumption) and unknown or unmodeled disturbances (e.g., solar and magnetic torque effects), as well as considering flexible spacecrafts (Zhu, Guo, Qiao, & Li, 2019).

Bibliography

Bang, H., Lee, J.-S., & Eun, Y.-J. (2004a). Nonlinear attitude control for a rigid spacecraft by feedback linearization. *KSME International Journal*, *18*(2), 203–210. https://doi.org/10.1007/BF03184729

Bang, H., Lee, J. S., & Eun, Y. J. (2004b). Nonlinear attitude control for a rigid spacecraft by feedback linearization. *KSME International Journal*, *18*(2), 203–210. https://doi.org/10.1007/BF03184729

Byrnes, C. I., & Isidori, A. (1991). On the attitude stabilization of rigid spacecraft. *Automatica*, *27*(1), 87–95.

[1] Note that the control law in (Jin, Ko, & Ryoo, 2008) is designed to track a trajectory defined in terms of Modified Rodriguez Parameters (MRP), but, with trivial transformations it is possible to report the simulation results in the error quaternion attitude representation.

https://doi.org/10.1016/0005-1098(91)90008-P
Fresk, E., & Nikolakopoulos, G. (2013). *Full Quaternion Based Attitude Control for a Quadrotor*. https://doi.org/10.0/Linux-x86_64
Ghiglino, P., Forshaw, J. L., & Lappas, V. J. (2015). OQTAL: Optimal quaternion tracking using attitude error linearization. *IEEE Transactions on Aerospace and Electronic Systems*, *51*(4), 2715–2731. https://doi.org/10.1109/TAES.2015.140219
Goldstein, H., Poole, C., Safko, J., & Addison, S. R. (2002). Classical mechanics. *American Journal of Physics*, *70*, 782. https://doi.org/10.1016/0029-5582(61)90325-X
Grubin, C. (1970). Derivation of the Quaternion Scheme via the Euler Axis and Angle. *Journal of Spacecraft and Rockets*, *7*(October), 1261–1263. https://doi.org/10.2514/3.30149
Isidori, A. (1995). *Nonlinear Control Systems*. London: Springer London. https://doi.org/10.1007/978-1-84628-615-5
Ismail, Z., & Varatharajoo, R. (2010). A study of reaction wheel configurations for a 3-axis satellite attitude control. *Advances in Space Research*. https://doi.org/10.1016/j.asr.2009.11.004
Jin, J., Ko, S., & Ryoo, C.-K. (2008). Fault tolerant control for satellites with four reaction wheels. *Control Engineering Practice*, *16*(10), 1250–1258. https://doi.org/10.1016/J.CONENGPRAC.2008.02.001
Kaplan, M. H. (1976). *Modern spacecraft dynamics and control*. Wiley.
Liou, J.-C. (2006). PLANETARY SCIENCE: Risks in Space from Orbiting Debris. *Science*, *311*(5759), 340–341. https://doi.org/10.1126/science.1121337
Lizarralde, F., & Wen, J. T. (1996). Attitude control without angular velocity measurement: a passivity approach. *IEEE Transactions on Automatic Control*, *41*(3), 468–472. https://doi.org/10.1109/9.486654
Lo, S.-C., & Chen, Y.-P. (1995). Smooth sliding-mode control for spacecraft attitude tracking maneuvers. *Journal of Guidance, Control, and Dynamics*, *18*(6), 1345–1349. https://doi.org/10.2514/3.21551
Long-Life Show, Jyh-Ching Juang, Chen-Tsung Lin, & Ying-Wen Jan. (2002). Spacecraft robust attitude tracking design: PID control approach. In *Proceedings of the 2002 American Control Conference (IEEE Cat. No.CH37301)* (pp. 1360–1365 vol.2). IEEE. https://doi.org/10.1109/ACC.2002.1023210
Markley, F. L., & Crassidis, J. L. (2014). *Fundamentals of Spacecraft Attitude Determination and Control*. Springer, New York, NY. https://doi.org/10.1007/978-1-4939-0802-8
Mehra, R., Seereeram, S., Bayard, D., & Hadaegh, F. (2002). Adaptive Kalman filtering, failure detection and identification for spacecraft attitude estimation. In *Proceedings of International Conference on Control Applications* (pp. 176–181). IEEE. https://doi.org/10.1109/cca.1995.555664
Navabi, M., & Hosseini, M. R. (2017). Spacecraft quaternion based attitude input-output feedback linearization control using reaction wheels. In *2017 8th International Conference on Recent Advances in Space Technologies (RAST)* (pp. 97–103). IEEE. https://doi.org/10.1109/RAST.2017.8002994
Reyes-Valeria, E., Enriquez-Caldera, R., Camacho-Lara, S., & Guichard, J. (2013). LQR control for a quadrotor using unit quaternions: Modeling and simulation. In *CONIELECOMP 2013, 23rd International Conference on Electronics, Communications and Computing* (pp. 172–178). IEEE. https://doi.org/10.1109/CONIELECOMP.2013.6525781
Tregouet, J.-F., Arzelier, D., Peaucelle, D., Pittet, C., & Zaccarian, L. (2015). Reaction Wheels Desaturation Using Magnetorquers and Static Input Allocation. *IEEE Transactions on Control Systems Technology*, *23*(2), 525–539. https://doi.org/10.1109/TCST.2014.2326037
Wang, Q., Yuan, J., & Zhu, Z. (2005). The application of error quaternion and PID control method in Earth observation satellite's attitude control system. In *Systems and Control in Aerospace and Astronautics, 2006. ISSCAA 2006. 1st International Symposium on* (pp. 128–131). IEEE. https://doi.org/10.1109/ISSCAA.2006.1627596
Wen, J. T.-Y., & Kreutz-Delgado, K. (1991). The attitude control problem. *IEEE Transactions on Automatic Control*, *36*(10), 1148–1162. https://doi.org/10.1109/9.90228
Wie, B., & Barba, P. M. (1985). Quaternion feedback for spacecraft large angle maneuvers. *Journal of Guidance, Control, and Dynamics*, *8*(3), 360–365. https://doi.org/10.2514/3.19988
Xiao, B., Hu, Q., & Zhang, Y. (2012). Adaptive sliding mode fault tolerant attitude tracking control for flexible spacecraft under actuator saturation. *IEEE Transactions on Control Systems Technology*, *20*(6), 1605–1612. https://doi.org/10.1109/TCST.2011.2169796
Yang, Y. (2017). Spacecraft Attitude and Reaction Wheel Desaturation Combined Control Method. *IEEE Transactions on Aerospace and Electronic Systems*, *53*(1), 286–295. https://doi.org/10.1109/TAES.2017.2650158
Zhou, K., Doyle, J. C., & Glover, K. (Keith). (1996). *Robust and optimal control*. Prentice Hall.
Zhu, Y., Guo, L., Qiao, J., & Li, W. (2019). An enhanced anti-disturbance attitude control law for flexible spacecrafts subject to multiple disturbances. *Control Engineering Practice*, *84*, 274–283. https://doi.org/10.1016/j.conengprac.2018.11.001
Zipfel, P. H. (2007). *Modeling and Simulation of Aerospace Vehicle Dynamics, Second Edition*. Reston ,VA: American Institute of Aeronautics and Astronautics. https://doi.org/10.2514/4.862182
Zou, A.-M., & Kumar, K. D. (2011). Adaptive fuzzy fault-tolerant attitude control of spacecraft. *Control Engineering Practice*, *19*(1), 10–21. https://doi.org/10.1016/J.CONENGPRAC.2010.08.005